ACS Medicinal Chemistry Letters

pubs.acs.org/acsmedchemlett Letter

Discovery of a Pyrimidothiazolodiazepinone as a Potent and Selective Focal Adhesion Kinase (FAK) Inhibitor

Brian J. Groendyke,[#] Behnam Nabet,[#] Mikaela L. Mohardt, Haisheng Zhang, Ke Peng, Eriko Koide, Calvin R. Coffey, Jianwei Che, David A. Scott, Adam J. Bass, and Nathanael S. Gray*

Cite This: ACS Med. Chem. Lett. 2021, 12, 30−38 Read Online

ACCESS | Metrics & More | Article Recommendations | Supporting Information

ABSTRACT: Focal adhesion kinase (FAK) is a tyrosine kinase with prominent roles in protein scaffolding, migration, angiogenesis, and anchorage-independent cell survival and is an attractive target for the development of cancer therapeutics. However, current FAK inhibitors display dual kinase inhibition and/or significant activity on several kinases. Although multitargeted activity is at times therapeutically advantageous, such behavior can also lead to toxicity and confound chemical-biology studies. We report a novel series of small molecules based on a tricyclic pyrimidothiazolodiazepinone core that displays both high potency and selectivity for FAK. Structure−activity relationship (SAR) studies explored modifications to the thiazole, diazepinone, and aniline "tail," which identified lead compound BJG-03-025. BJG-03-025 displays potent biochemical FAK inhibition (IC_{50} = 20 nM), excellent kinome selectivity, activity in 3D-culture breast and gastric cancer models, and favorable pharmacokinetic properties in mice. BJG-03-025 is a valuable chemical probe for evaluation of FAK-dependent biology.

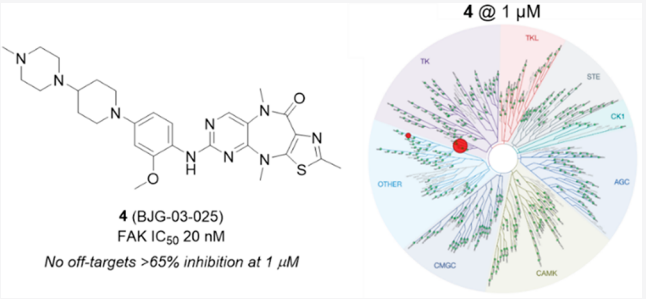

KEYWORDS: *FAK, selective inhibitors, structure−activity relationships, aminothiazole, anticancer agents*

Focal adhesion kinase (FAK, also known as protein tyrosine kinase 2 [PTK2]) is a tyrosine kinase with important roles in reorganizing actin and focal adhesions, coordinating PI3K-AKT and integrin signaling networks, and regulating nuclear gene expression programs. In the context of cancer, FAK plays prominent kinase-dependent and kinase-independent roles in coordinating migration, angiogenesis, and anchorage-independent cell survival.[1] FAK is commonly overexpressed or amplified in many cancers, including ovarian, breast, colorectal, and pancreatic cancers. We recently demonstrated that FAK coordinates YAP/TAZ, PI3K-AKT, and β-catenin signaling in diffuse gastric cancer.[2] For these reasons, targeted disruption of FAK has been of great interest and a number of potent FAK inhibitors have been developed and advanced to clinical trials. While FAK inhibition has been tolerable and leads to cytostatic effects, single-agent clinical efficacy of FAK inhibitors is limited.[3] Combination approaches with FAK inhibitors are under active investigation. For example, FAK inhibitors have been shown to sensitize pancreatic cancer to chemotherapy or checkpoint inhibitors,[4] leading to several ongoing clinical trials.[5]

Many of the existing FAK inhibitors, such as defactinib (VS-6063),[6] VS-4718 (PND-1186),[7] PF-573228,[8] CEP-37440,[9] and TAE226,[10] share a 2,4-diaminopyrimidine or 2,4-diaminopyridine motif (Figure 1). These compounds are highly potent ATP-competitive kinase inhibitors, with biochemical IC_{50} values in the single-digit nanomolar range but display either dual kinase inhibition or significant activity against other kinases. Several bicyclic scaffolds, namely, 7-azaindoles,[11] pyrrolopyrimidines,[12] and imidazotriazines,[13] have delivered potent (IC_{50} < 50 nM) FAK inhibitors, but the full kinome profiles of these series are not reported. Although off-target activity is at times therapeutically advantageous,[14,15] off-target effects from nonselective probes can confound chemical-biology studies. In this study, we describe the identification and characterization of a highly selective FAK inhibitor, BJG-03-025. BJG-03-025 is based on a privileged benzopyrimidodiazepinone core scaffold which we have elaborated previously to target kinases including: ERK5,[16] PI3Kδ,[17] TNK2,[18] and nonkinases such as BRD4.[19] BJG-03-025 was identified following a systematic structure−activity relationship campaign after observing serendipitous selectivity for this scaffold class from kinome-wide profiling studies. We observe that BJG-03-025 displays antiproliferative activity in three-dimensional (3D)-breast and gastric cancer models and

Received: June 18, 2020
Accepted: November 18, 2020
Published: December 14, 2020

https://dx.doi.org/10.1021/acsmedchemlett.0c00338
ACS Med. Chem. Lett. 2021, 12, 30−38

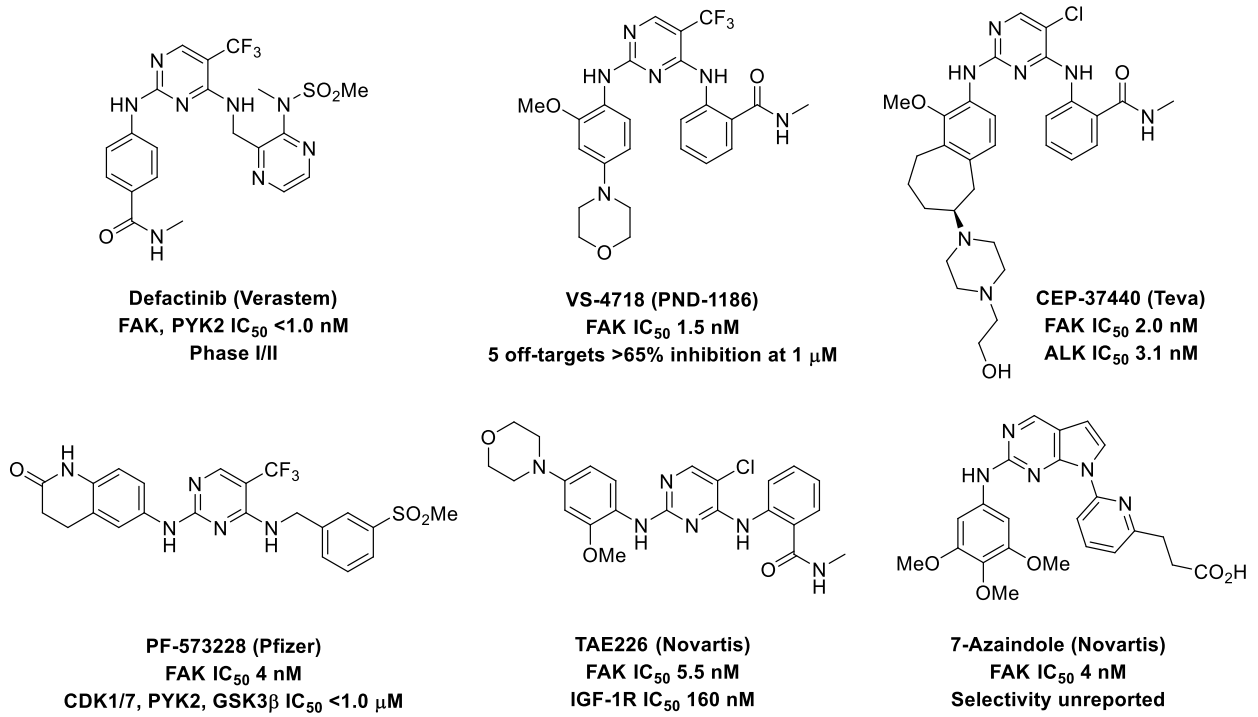

Figure 1. Existing FAK inhibitors are potent but display multikinase activity.

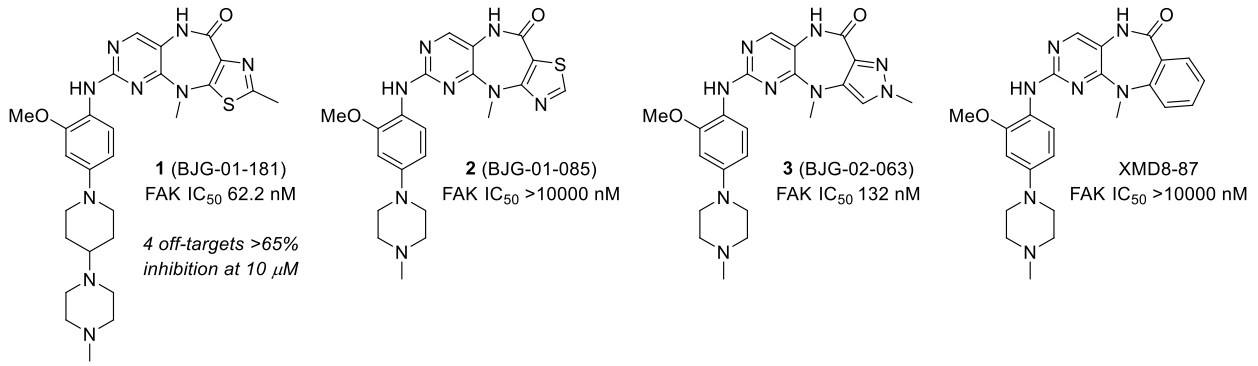

Figure 2. Identification of **1** (BJG-01-181), a highly selective FAK inhibitor and chemical structures of related analogues.

impacts cellular signaling and migration. Our selective FAK inhibitor is a valuable probe for evaluation of FAK-specific biology.

Previous work in our group has shown the tricyclic benzopyrimidodiazepinone core to be a privileged scaffold for the design of potent and selective kinase inhibitors. During a campaign to replace the benzene of the benzopyrimidodiazepinone core with heteroaryl rings, KINOME*scan* profiling revealed **1** (BJG-01-181) as an exceptionally selective FAK inhibitor, displaying >65% inhibition of only 5 out of 402 kinases at a testing concentration of 10 μM (Figures 2 and S1, Table S1). A biochemical kinase assay confirmed **1** as a moderately potent FAK inhibitor (IC_{50} = 62.2 nM); although less potent than other FAK inhibitors, **1** is notably more selective (Table S2). From this starting point, we explored the structure−activity relationships (SAR) of this novel scaffold to improve FAK potency and better understand the source of its kinome selectivity.

A comparison of **1** with a structurally similar thiazole isomer (**2**, FAK IC_{50} > 10 000 nM) revealed that the thiazole nitrogen must be in the "top" position, adjacent to the diazepinone carbonyl (Figure 2). We surmised that this nitrogen may provide an important hydrogen-bonding interaction. The closely related pyrazole **3** displayed similar FAK potency (IC_{50} = 132 nM), lending further support to this hypothesis. For other members of the pyrimidodiazepinone series, amide *N*-methylation often leads to increased potency due to a beneficial interaction with the gatekeeper residue.[20,21] Furthermore, the N-methylated compounds generally possess better pharmacokinetic (PK) properties than the secondary amides.[18] Compound **4** (BJG-03-025), an *N*-methyl matched-pair with **1**, was synthesized and showed a 3-fold improvement, with a FAK IC_{50} of 20.2 ± 1.9 nM. Further optimization focused on the N-methylated tricyclic core. SAR studies to investigate the effects of different aniline "tails" and substitution at the tricyclic core were conducted in parallel (Table 1). To enable direct comparisons, aniline screening was conducted using the 2-methyl thiazole core **10**. Similarly, to interrogate the effects of substitution patterns on the tricyclic

https://dx.doi.org/10.1021/acsmedchemlett.0c00338
ACS Med. Chem. Lett. 2021, 12, 30−38

Table 1. Structure–Activity Relationships of the Aniline Component

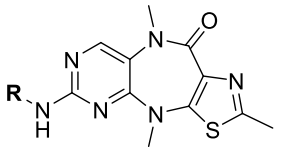

4, 11-28

Cmpd	R	FAK IC_{50} (μM)[a]	Cell IC_{50} (μM)[b]	Cmpd	R	FAK IC_{50} (μM)[a]	Cell IC_{50} (μM)[b]
4	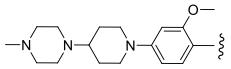	0.020±0.002[c]	3.6	**20**	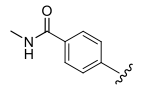	0.173±0.009	5.9
11	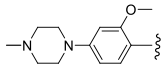	0.030±0.001	2.3	**21**	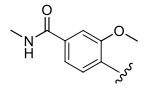	0.045±0.002	>10
12	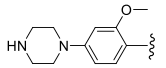	0.044±0.001	2.5	**22**	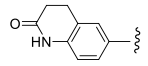	0.670±0.013	>10
13	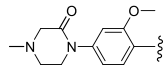	0.082±0.002	N.D.	**23**	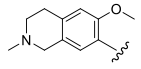	0.038±0.002	>10
14	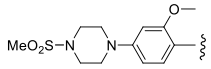	0.047±0.003	>10	**24**	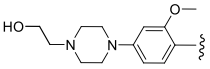	0.074±0.002	>10
15	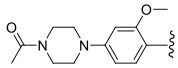	0.046±0.002	N.D.	**25**	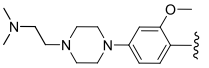	0.067±0.003	N.D.
16	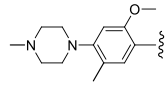	0.032±0.001	7.7	**26**	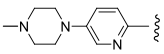	0.196±0.011	N.D.
17	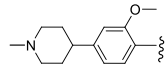	0.052±0.002	3.7	**27**		0.666±0.049	N.D.
18	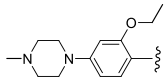	0.055±0.001	6.1	**28**	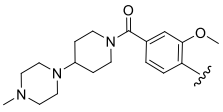	0.078±0.004	>10
19	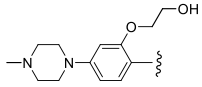	0.465±0.032	N.D.				

[a]IC_{50} measured using the Z'LYTE assay (ThermoFisher Scientific), as duplicate experiments. [b]IC_{50} of viability of MDA-MB-231 cells in ultra-low adherent 3D-spheroid suspensions. Values are derived from data presented in Figures 5B and S8 and are representative of $n = 3$ independent experiments. N.D., not determined. [c]$n = 4$, two independent batches each tested in duplicate.

core, the 2-methoxy-4-(4-(4-methylpiperazinyl)piperidinyl) aniline was used in all examples.

Tricyclic core **10** can be obtained via the synthetic scheme shown in Scheme 1. Other analogues were prepared using the same synthetic sequence, or with slight modifications (see the Supporting Information (SI) for details). Commercially available ethyl 2-methylthiazole-4-carboxylate **5** was brominated with N-bromosuccinimide (NBS) to afford bromothiazole **6**. Palladium-catalyzed amination with benzophenone imine, followed by hydrolysis provided primary amine **7** in good yield. Deprotonation of the primary amine and treatment with iodomethane provided *N*-methyl **8**. All attempts to forge the thiazole C5–N bond via nitration of **5** or S_NAr reaction of **6** were unsuccessful. N-Arylation of **8** with 2,4-dichloro-5-nitropyrimidine under NaH conditions provided intermediate **9**, which was subjected to an iron-promoted reductive cyclization and subsequent methylation with iodomethane to provide the tricyclic core **10**. The final compounds were prepared by Buchwald–Hartwig amination with the corresponding aniline or heterocyclic amine.

Modification of the solvent-exposed side chain aimed to improve the potency of **4** while maintaining high kinome selectivity. We targeted several key residues in the solvent-exposed channel, including Arg426, Gln438, and Glu506 (Figure 3), by incorporating hydrogen-bond donors or acceptors into the aniline tail. A variety of modifications yielded inhibitors with biochemical IC_{50}s in the 30–60 nM range (Table 1), but did not improve upon the potency of **4**. In contrast, several side chains, such as hydroxyethyl ether **19**, tetrahydroquinolinone **22**, and pyrazole **27**, were not tolerated and resulted in lower biochemical potency.

https://dx.doi.org/10.1021/acsmedchemlett.0c00338
ACS Med. Chem. Lett. 2021, 12, 30–38

Scheme 1. Synthesis of 4 and 11−28[a]

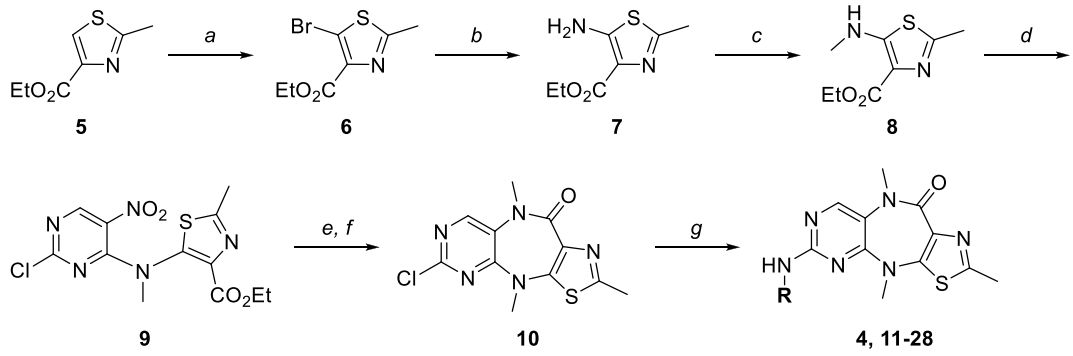

[a]Reagents and conditions: (a) NBS, acetonitrile, 40 °C, 61%. (b) (i) Pd_2 $(dba)_3$, BINAP, Cs_2CO_3, benzophenone imine, toluene, 80 °C, (ii) THF/1 M aq HCl (4:1 mixture), rt, 68% over two steps. (c) NaH, MeI, THF, 0 °C to rt, 41%. (d) NaH, 2,4-dichloro-5-nitropyrimidine, THF, 0 °C to rt, 59%. (e) Fe, glacial acetic acid, 50 °C. (f) NaH, MeI, DMF, 0 °C to rt, 48% over two steps. (g) Pd_2 $(dba)_3$, XPhos, K_2CO_3, amine, *t*-BuOH 100 °C.

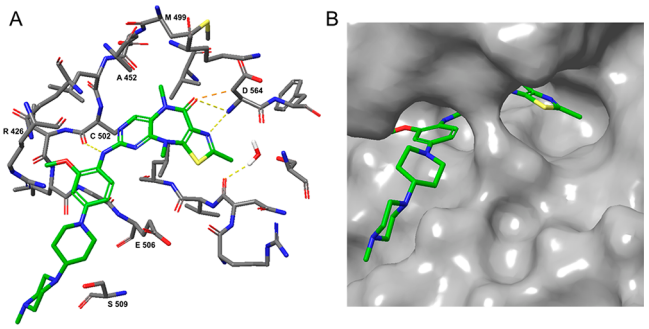

Figure 3. Docking of **4** with FAK (PDB 6I8Z). (A) Key interactions of **4** with active-site residues, notably the critical hydrogen-bond of the thiazole nitrogen with Asp564. (B) FAK surface map shows the U-shaped active site, with the 2-methyl group extending into a hydrophobic pocket.

Our observation that the opposite thiazole isomer (i.e., **2**) was inactive suggested that the steric and electronic properties of the tricyclic core had a significant effect on the ability to bind FAK. We turned to molecular modeling to gain further insight into the binding mode of **4** and how its potency could be improved (Figure 3). Docking of **4** with FAK (PDB: 6I8Z) revealed two hydrogen-bonding interactions: binding to hinge Cys502 via the aminopyrimidine and binding to the side-chain of Asp564, part of the DFG motif, via the diazepinone carbonyl and thiazole nitrogen. The loss of potency observed for thiazole isomer **2** is likely due to the loss of this hydrogen-bonding interaction. Providing further support for this hypothesis, related benzopyrimidodiazepinones such as XMD8-87 (Figure 2) do not engage FAK.[18] The *N*-methyl amide extends toward the top of the FAK cavity, potentially interacting with Ala452 (Figure 3A); however, it was uncertain whether further modifications would be tolerated. The thiazole 2-methyl extends into the back pocket of the FAK active site, and we hypothesized that longer substituents at this position might benefit from hydrophobic interactions (Figure 3B). Similarly, we proposed that longer substituents on the "bottom" nitrogen of the central ring could extend out of the back end of the U-shaped binding site, potentially gaining beneficial hydrophobic contacts (Figure 3B). Docking analyses of **3**, **20**, and **26** predicted the same binding mode as **4** (Figure S6).

A summary of SAR studies on the tricyclic core is presented in Table 2. Removal of the thiazole 2-methyl (**29**) decreased potency roughly 8-fold compared to **1** (IC_{50} 510 vs 62 nM). However, larger substituents at the thiazole 2-position were met with mixed success: ethyl- and isopropyl-substituted analogues **30** and **31** retained activity against FAK, but a phenyl group was not tolerated (**32**). Whereas N-ethylation at either position of the central ring (**34**, **35**) retained nearly identical potency to **4**, other substitutions of the bottom nitrogen led to a slight loss in potency (**36**, **37**). Introduction of an electron-withdrawing group (2-CF_3 **33**, oxazole **38**) sharply decreased potency, further highlighting the importance of the hydrogen bond between the thiazole and Asp564. Interestingly, while **38** is predicted to bind in the same manner as **4**, docking of **37** revealed a puckered conformation of the central ring to accommodate the longer *N*-propyl group (Figure S6).

Table 2. Structure−Activity Relationships of the Tricyclic Core

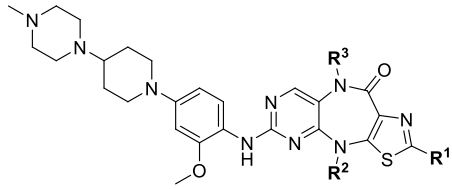

4, 29-38

compd	R^1	R^2	R^3	FAK IC_{50} (μM)[a]	cell IC_{50} (μM)[b]
4	CH_3	CH_3	CH_3	0.020 ± 0.002[c]	3.6
29	H	CH_3	H	0.510 ± 0.035	ND
30	Et	CH_3	CH_3	0.032 ± 0.001	ND
31	*i*-Pr	CH_3	CH_3	0.059 ± 0.001	ND
32	Ph	CH_3	CH_3	>10	ND
33	CF_3	CH_3	CH_3	0.134 ± 0.001	ND
34	CH_3	CH_3	Et	0.019 ± 0.001	0.93
35	CH_3	Et	CH_3	0.023 ± 0.001	>10
36	CH_3	CH_2CF_3	CH_3	0.068 ± 0.002	ND
37	CH_3	*n*-Pr	CH_3	0.047 ± 0.001	ND
38[d]	CH_3	CH_3	CH_3	0.525 ± 0.016	>10

[a]IC_{50} measured using the Z'LYTE assay (ThermoFisher Scientific), as duplicate experiments. [b]IC_{50} of viability of MDA-MB-231 cells in ultra-low adherent 3D-spheroid suspensions. Values are derived from data presented in Figures 5B and S8 and are representative of $n = 3$ independent experiments. ND, not determined. [c]$n = 4$, two independent batches each tested in duplicate. [d]Oxazole instead of thiazole.

https://dx.doi.org/10.1021/acsmedchemlett.0c00338
ACS Med. Chem. Lett. 2021, 12, 30−38

With **4** selected as the lead compound, its kinome selectivity was profiled by KINOME*scan* screening to confirm that amide N-methylation does not ablate the selectivity initially observed with **1** (Figure 4, Table S1). Although a few additional kinase

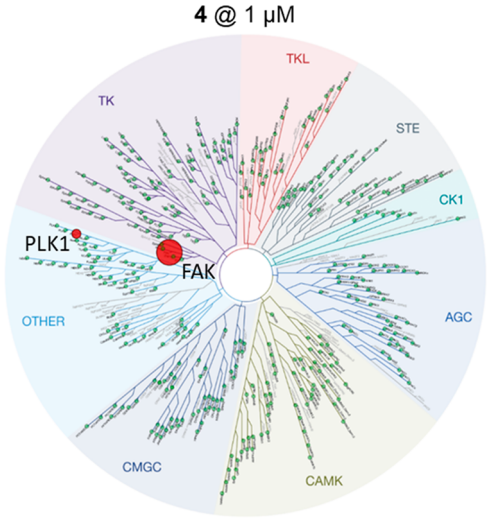

Figure 4. KINOME*scan* profile of **4**.

targets are registered at a 10 μM screening concentration (Figure S2, Table S1), **4** displays "complete" selectivity for FAK at a screening concentration of 1 μM, with an S(35) score of 0.01. In comparison, at an identical screening concentration the S(35) score for defactinib is 0.24.[22] Biochemical IC_{50}s were obtained for all nonmutant kinases registering <35% control in the 10 μM KINOME*scan* assay (Figure S2), demonstrating that **4** is approximately 100−300-fold selective for FAK. PLK1 proved to be a false positive, with an enzyme IC_{50} of 8.3 μM, and no cell-cycle disruption was observed during in vitro profiling.

Seven compounds from the 2-methylthiazole series were evaluated in a mouse-liver microsome stability assay (Table S6). All compounds demonstrated good to excellent microsome stability, with half-lives ranging from 25.5 to >120 min. Lead compound **4** was then submitted for further pharmacokinetic (PK) profiling in mice, with IV (2 mg/kg) and PO (10 mg/kg) doses administered. As shown in Table 3, **4** exhibits

Table 3. Mouse Pharmacokinetic Parameters for 4

dose	parameter	4
2 mg/kg IV	CL (mL/min/kg)	18.5
	$t_{1/2}$ (h)	5.29
	V_{ss} (L/kg)	4.07
10 mg/kg PO	C_{max} (μM)	0.42
	T_{max} (h)	4.00
	AUC_{inf} (h·μg/mL)	1.82
	F (%)	18.3

low clearance (18.5 mL/min/kg) and is metabolically stable, displaying an average $t_{1/2}$ of 5.29 h under IV administration. For both routes, detectable levels of drug were observed 24 h after dosing (Tables S7, S8; Figures S4, S5). However, oral bioavailability is limited (%F = 18).

We next aimed to explore the biological activity of our FAK inhibitor series. *PTK2*, the gene that encodes FAK, is a significant genetic dependency in pan-cancer cell line analysis including breast, colorectal, and gastric cancer models (Cancer Dependency Map)[23] (Figure S7). We selected MDA-MB-231 cells as a versatile cell line to explore FAK-dependent phenotypes due to their high genetic dependence and overexpression of *PTK2* (Figure S7D). Prior studies also indicate that these MDA-MB-231 cells display FAK-dependent migration and invasion potential.[24,25] For high-throughput evaluation of the biological effects of our compound series, we compared antiproliferative effects of defactinib, VS-4718, and PF-573228 to 17 representative compounds from our series upon treatment of MDA-MB-231 cells in two-dimensional (2D)-monolayer cultures and ultra-low adherent (ULA) three-dimensional (3D)-spheroid suspensions. We and others have also previously shown that 3D-spheroids serve as better model systems to evaluate drug sensitivity and in vivo tumor physiology.[20,26−28] In addition, published FAK agents have limited activity in 2D-monolayer cultures and studies demonstrate improved activity in 3D-culture and in vivo models potentially due to FAK's kinase-dependent and kinase-independent roles in integrin signaling, adhesion and protein scaffolding.[7,29,30]

Across the compound series, we observed that MDA-MB-231 cells were more sensitive to FAK inhibition in 3D-spheroids, consistent with prior studies (Figures 5A,B and S8; Tables 1 and 2). VS-4718, defactinib, and PF-573228, which display the most pronounced biochemical potency on FAK, also had the most pronounced antiproliferative effects likely due to a combination of direct FAK inhibitory activity combined with potential multikinase activities. Of our series, **4**, **11**, **12**, **17**, and **34** displayed the most pronounced antiproliferative effects in 3D-spheroids, with little to no effects in 2D-monolayer cultures.

In general, the SAR trends observed for biochemical potency of our series largely translate to activity in 3D-spheroids. For example, **24** and **28** are ∼4-fold less potent than **4** and are >3-fold less potent in the 3D assay. Likewise, **22** shows only modest biochemical potency and does not inhibit proliferation. One exception is the matched pair **20** and **21**, where the 2-methoxy **21** is more potent biochemically but demonstrates weaker antiproliferation. This weaker phenotype may stem from a reduced off-target profile that is frequently observed for 2-methoxyanilines.[18] Notably, **34**, **4**, and **35** elicit different biological activity despite possessing nearly identical biochemical potencies. These three compounds have similar kinetic and thermodynamic solubilities, show moderate permeability in a Caco-2 assay, and are potential substrates of P-glycoprotein (P-gp; Tables S8−S10). The improved antiproliferative effect of **34** relative to **4** may stem from the better permeability ($P_{app,A\rightarrow B}$ 83 vs 58 nm/s) and lower efflux ratio (2.2 vs 4.1, respectively) of **34**. At present, it remains unclear as to why several compounds, such as **14**, **16**, **23**, and **35** display little activity in 3D-spheroids despite being potent biochemical inhibitors.

We further evaluated the effects of **4** on the ability of MDA-MB-231 cells to migrate in response to chemoattraction (serum-containing media). Treatment with **4** led to a statistically significant albeit modest effect on migration of MDA-MB-231 cells. These effects were more pronounced upon treatment with defactinib and nocodazole, an agent that disrupts microtubule polymerization[31] (Figures 5C and S9). Together, these data indicate that selective FAK inhibition with **4** leads to modest loss of viability in 3D-suspensions and migratory potential of MDA-MB-231 cells.

https://dx.doi.org/10.1021/acsmedchemlett.0c00338
ACS Med. Chem. Lett. 2021, 12, 30−38

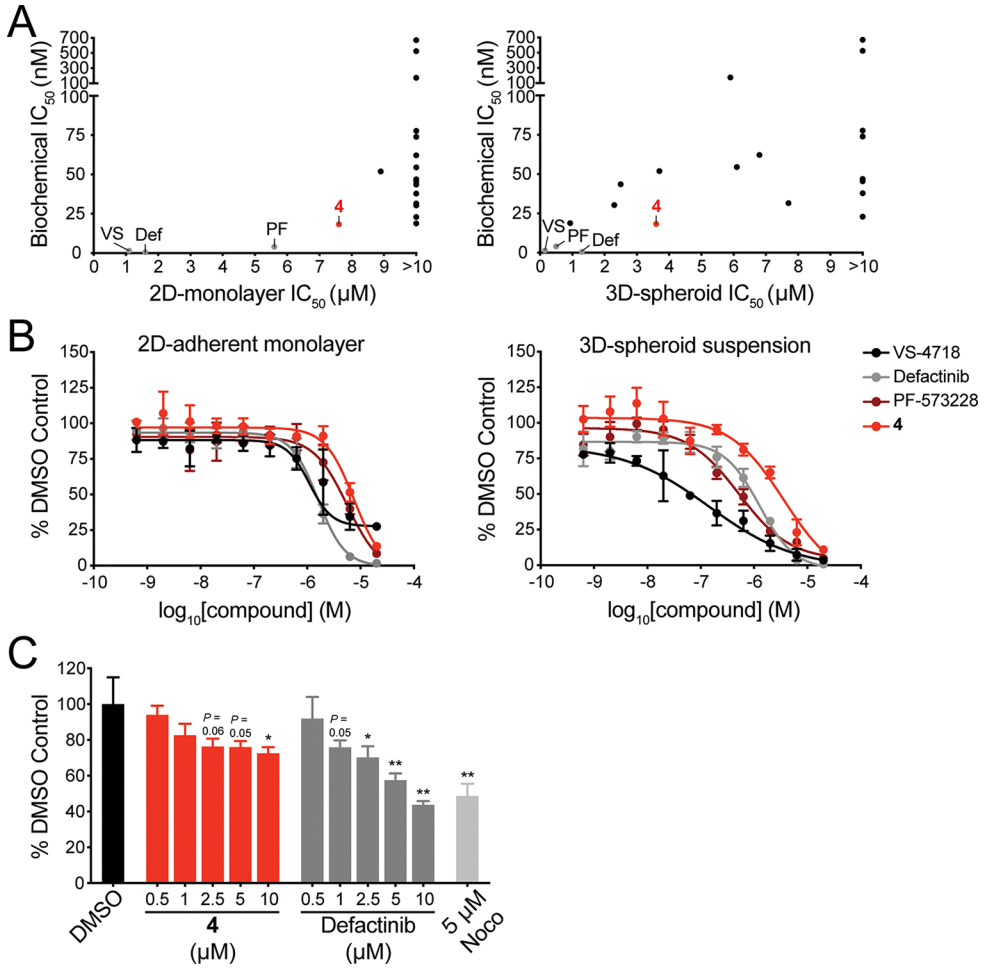

Figure 5. FAK inhibition decreases proliferation in 3D-spheroid suspensions and migration of breast cancer cells. (A) Scatterplot depicting biochemical IC_{50} compared to cellular IC_{50} upon treatment of MDA-MB-231 cells cultured as 2D-adherent monolayers (left plot) or ultra-low adherent 3D-spheroid suspensions (right plot). VS-4718 (VS), defactinib (Def), and PF-573228 (PF) are noted in gray, **4** is noted in red, and the pyrimidothiazolodiazepinone series is noted in black. (B) DMSO-normalized antiproliferation of MDA-MB-231 cells treated with the indicated compounds for 120 h. Cells were cultured as 2D-adherent monolayers (left plot) or ultra-low adherent 3D-spheroid suspensions (right plot). Data are presented as mean ± SD of $n = 4$ biologically independent samples and are representative of $n = 3$ independent experiments. (C) DMSO-normalized migration of MDA-MB-231 cells after 24 h under the indicated conditions (nocodazole, Noco). Representative images are provided in Figure S9. Data are presented as mean ± SD of $n = 3$ biologically independent samples and are representative of $n = 3$ independent experiments. *P* values were derived from a two-tailed Student's *t* test compared to DMSO control are noted (*$P < 0.05$, **$P < 0.01$).

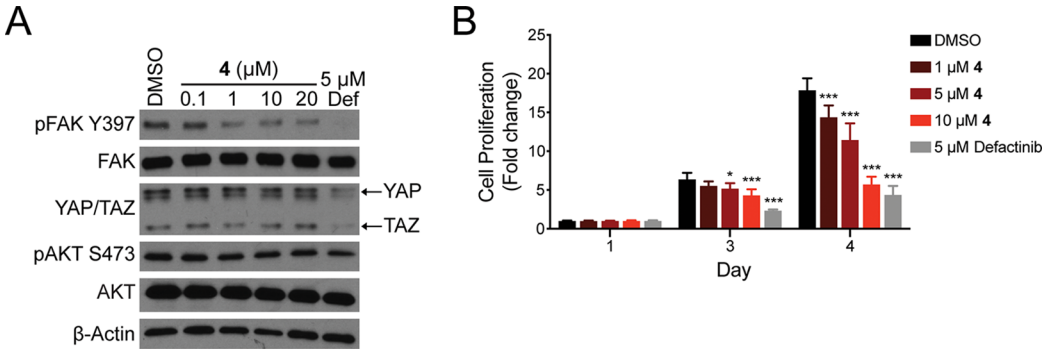

Figure 6. FAK inhibition decreases aberrant signaling and proliferation of gastric cancer organoids. (A) Immunoblot analysis of *CDH1*$^{-/-}$ *RHOA*$^{Y42C/+}$ gastric organoids treated with DMSO, **4**, or defactinib at the indicated concentrations for 24 h. Data are representative of $n = 3$ independent experiments. (B) Relative proliferation of *CDH1*$^{-/-}$ *RHOA*$^{Y42C/+}$ gastric organoids treated with DMSO, **4**, or defactinib (Def) at the indicated concentrations for the indicated time-course. Data are presented as mean ± SD of $n = 7–10$ biologically independent samples and are representative of $n = 3$ independent experiments. *P* values were derived from a two-tailed Student's *t* test compared to DMSO control are noted (*$P < 0.05$, ***$P < 0.001$).

https://dx.doi.org/10.1021/acsmedchemlett.0c00338
ACS Med. Chem. Lett. 2021, 12, 30−38

To corroborate these findings, we evaluated the effects of FAK inhibition in HT-29 cells, a colorectal adenocarcinoma cell line with *PTK2* copy number alterations and elevated expression levels (Figures S7D and S10A). Treatment with **4** led to little or no activity in 2D-monolayer or 3D-suspensions, while more pronounced antiproliferative activity was observed upon treatment with VS-4718, defactinib, and PF-573228 (Figure S10B). While the modest results achieved with **4** are consistent with a prior study evaluating FAK inhibition in HT-29 cells in 2D-monolayer culture and in vivo,[32] further testing of potential drug combination strategies may be necessary to achieve enhanced viability effects. For example, combination studies with vemurafenib may be warranted, which has been shown to synergize with FAK inhibitors in these *BRAF* mutant cells.[32]

To explore the effects of FAK inhibition in an additional translationally relevant biological context, we assayed the consequences of FAK inhibition in a gastric cancer $CDH1^{-/-}$ $RHOA^{Y42C/+}$ organoid model. We recently demonstrated that FAK, through activation of YAP/TAZ, PI3K/AKT and β-catenin signaling, coordinates diffuse gastric cancer progression.[2] Treatment of gastric organoids with **4** led to loss of active, phosphorylated FAK (pFAK Y397), which was more pronounced with defactinib after 24 h (Figure 6A). Defactinib treatment resulted in changes in active, phosphorylated AKT (pAKT S473) and total YAP/TAZ levels, consistent with our prior findings within 24 h,[2] while modest effects on pAKT S473 and active, nonphosphorylated YAP were observed with **4** after 48 h treatment (Figures 6A and S11). Differences in pathway responses corresponded with levels of antiproliferative activity. Treatment with **4** led to dose-dependent activity on gastric organoid proliferation, which was more pronounced with defactinib treatment (Figure 6B). Together, these results confirm the potential of targeted FAK inhibition in diffuse gastric cancer.

In summary, we describe the identification and characterization of a selective FAK inhibitor, **4**, and we disclose a novel tricyclic core bearing a substituted thiazole. We observe that FAK inhibition leads to loss of viability in breast and gastric cancer 3D-culture model systems, as well as effects on cellular signaling and migration. These effects are milder compared to published FAK inhibitors, in which enhanced effects may be due to additional activities on other kinases. Despite its milder phenotype, **4** may be particularly beneficial as a chemical probe when used in tandem with another kinase inhibitor to study the signaling effects and drug synergy upon dual inhibition, where a clean kinome profile is imperative. As **4** possesses suitable PK properties for studies in mice, further evaluation is required to examine whether the effects in 3D-culture models translate to efficacy in vivo. Our chemical probe serves as a valuable tool to explore the consequences of FAK inhibition and identify potential combination approaches in cancer.

■ ASSOCIATED CONTENT

Supporting Information

The Supporting Information is available free of charge at https://pubs.acs.org/doi/10.1021/acsmedchemlett.0c00338.

Details of biochemical and biological assays, synthetic procedures, and analytical data (PDF)

■ AUTHOR INFORMATION

Corresponding Author

Nathanael S. Gray − *Department of Cancer Biology, Dana-Farber Cancer Institute, Boston, Massachusetts 02115, United States; Department of Biological Chemistry and Molecular Pharmacology, Harvard Medical School, Boston, Massachusetts 02115, United States;* orcid.org/0000-0001-5354-7403; Email: nathanael_gray@dfci.harvard.edu

Authors

Brian J. Groendyke − *Department of Cancer Biology, Dana-Farber Cancer Institute, Boston, Massachusetts 02115, United States; Department of Biological Chemistry and Molecular Pharmacology, Harvard Medical School, Boston, Massachusetts 02115, United States;* orcid.org/0000-0002-3860-8308

Behnam Nabet − *Department of Cancer Biology, Dana-Farber Cancer Institute, Boston, Massachusetts 02115, United States; Department of Biological Chemistry and Molecular Pharmacology, Harvard Medical School, Boston, Massachusetts 02115, United States;* orcid.org/0000-0002-6738-4200

Mikaela L. Mohardt − *Department of Cancer Biology, Dana-Farber Cancer Institute, Boston, Massachusetts 02115, United States*

Haisheng Zhang − *Department of General Surgery, Nanfang Hospital, Southern Medical University, 510515 Guangzhou, China; Division of Molecular and Cellular Oncology, Dana-Farber Cancer Institute, Harvard Medical School, Boston, Massachusetts 02115, United States*

Ke Peng − *Division of Molecular and Cellular Oncology, Dana-Farber Cancer Institute, Harvard Medical School, Boston, Massachusetts 02115, United States*

Eriko Koide − *Department of Cancer Biology, Dana-Farber Cancer Institute, Boston, Massachusetts 02115, United States*

Calvin R. Coffey − *Department of Cancer Biology, Dana-Farber Cancer Institute, Boston, Massachusetts 02115, United States*

Jianwei Che − *Department of Cancer Biology, Dana-Farber Cancer Institute, Boston, Massachusetts 02115, United States; Department of Biological Chemistry and Molecular Pharmacology, Harvard Medical School, Boston, Massachusetts 02115, United States*

David A. Scott − *Department of Cancer Biology, Dana-Farber Cancer Institute, Boston, Massachusetts 02115, United States; Department of Biological Chemistry and Molecular Pharmacology, Harvard Medical School, Boston, Massachusetts 02115, United States;* orcid.org/0000-0003-3243-528X

Adam J. Bass − *Division of Molecular and Cellular Oncology, Dana-Farber Cancer Institute, Harvard Medical School, Boston, Massachusetts 02115, United States; Broad Institute of MIT and Harvard, Cambridge, Massachusetts 02142, United States*

Complete contact information is available at: https://pubs.acs.org/10.1021/acsmedchemlett.0c00338

Author Contributions

#B.J.G. and B.N. contributed equally to this work. B.J.G., B.N., and N.S.G. conceived of the study. B.J.G. led the medicinal chemistry study and performed compound synthesis and optimization. B.N. led and supervised the biological studies.

https://dx.doi.org/10.1021/acsmedchemlett.0c00338
ACS Med. Chem. Lett. 2021, 12, 30−38

B.N., M.L.M, H.Z., K.P., and E.K. performed biological assays. C.R.C. contributed to compound synthesis. J.C. performed docking modeling. D.A.S., A.J.B. and N.S.G. supervised the study. B.J.G. and B.N. wrote the manuscript, with edits from N.S.G. and D.A.S. All authors read and approved the manuscript.

Notes

The authors declare the following competing financial interest(s): FAK inhibitors noted in this study are subject to patent applications filed by Dana-Farber Cancer Institute. N.S.G. is a Scientific Founder, member of the SAB and equity holder in C4 Therapeutics, Syros, Soltego (board member), B2S, Allorion, Gatekeeper and Petra Pharmaceuticals. J.C. is a consultant for Soltego and equity holder of M3 bioinformatics & technology Inc. The Gray lab receives or has received research funding from Novartis, Takeda, Astellas, Taiho, Janssen, Kinogen, Voroni, Arbella, Deerfield and Sanofi. A.J.B receives funding from Bayer, Merck and Novartis and is a co-founder of Signet Therapeutics.

■ ACKNOWLEDGMENTS

We thank members of the Gray laboratory and S. Nabet for helpful discussions. This work was supported by an American Cancer Society Postdoctoral Fellowship PF-17-010-01-CDD (B.N.), Claudia Adams Barr Program in Innovative Basic Cancer Research Award (B.N.), Katherine L. and Steven C. Pinard Research Fund (N.S.G. and B.N.), V Foundation Translational Award (H.Z., K.P., and A.J.B.), NIH grant R01CA224428 (H.Z., K.P., and A.J.B.).

■ ABBREVIATIONS

AUC_{inf}, area under the curve extrapolated to infinity; CL, clearance; C_{max}, maximum concentration; F, bioavailability; IV, intravenous; PO, per os; $t_{1/2}$, half-life; T_{max}, time at C_{max}; V_{ss}, volume of distribution at steady state.

■ REFERENCES

(1) Sulzmaier, F. J.; Jean, C.; Schlaepfer, D. D. FAK in Cancer: Mechanistic Findings and Clinical Applications. *Nat. Rev. Cancer* **2014**, *14* (9), 598−610.

(2) Zhang, H.; Schaefer, A.; Wang, Y.; Hodge, R. G.; Blake, D. R.; Diehl, J. N.; Papageorge, A. G.; Stachler, M. D.; Liao, J.; Zhou, J.; Wu, Z.; Akarca, F.; De Klerk, L. K.; Derks, S.; Pierobon, M.; Hoadley, K. A.; Wang, T. C.; Church, G.; Wong, K. K.; Petricoin, E. F.; Cox, A. D.; Lowy, D. R.; Der, C. J.; Bass, A. J. Gain-of-Function RHOA Mutations Promote Focal Adhesion Kinase Activation and Dependency in Diffuse Gastric Cancer. *Cancer Discovery* **2020**, *10* (2), 288−305.

(3) Mohanty, A.; Pharaon, R. R.; Nam, A.; Salgia, S.; Kulkarni, P.; Massarelli, E. FAK-Targeted and Combination Therapies for the Treatment of Cancer: an Overview of Phase I and II Clinical Trials. *Expert Opin. Invest. Drugs* **2020**, *29* (4), 399−409.

(4) Jiang, H.; Hegde, S.; Knolhoff, B. L.; Zhu, Y.; Herndon, J. M.; Meyer, M. A.; Nywening, T. M.; Hawkins, W. G.; Shapiro, I. M.; Weaver, D. T.; Pachter, J. A.; Wang-Gillam, A.; DeNardo, D. G. Targeting Focal Adhesion Kinase Renders Pancreatic Cancers Responsive to Checkpoint Immunotherapy. *Nat. Med.* **2016**, *22* (8), 851−60.

(5) Symeonides, S. N.; Anderton, S. M.; Serrels, A. FAK-Inhibition Opens the Door to Checkpoint Immunotherapy in Pancreatic Cancer. *J. Immunother. Cancer* **2017**, *5*, 17.

(6) Shimizu, T.; Fukuoka, K.; Takeda, M.; Iwasa, T.; Yoshida, T.; Horobin, J.; Keegan, M.; Vaickus, L.; Chavan, A.; Padval, M.; Nakagawa, K. A First-in-Asian Phase 1 Study to Evaluate Safety, Pharmacokinetics and Clinical Activity of VS-6063, a Focal Adhesion Kinase (FAK) Inhibitor in Japanese Patients with Advanced Solid Tumors. *Cancer Chemother. Pharmacol.* **2016**, *77* (5), 997−1003.

(7) Tanjoni, I.; Walsh, C.; Uryu, S.; Tomar, A.; Nam, J. O.; Mielgo, A.; Lim, S. T.; Liang, C.; Koenig, M.; Patel, N.; Kwok, C.; McMahon, G.; Stupack, D. G.; Schlaepfer, D. D. PND-1186 FAK Inhibitor Selectively Promotes Tumor Cell Apoptosis in Three-Dimensional Environments. *Cancer Biol. Ther.* **2010**, *9* (10), 764−77.

(8) Slack-Davis, J. K.; Martin, K. H.; Tilghman, R. W.; Iwanicki, M.; Ung, E. J.; Autry, C.; Luzzio, M. J.; Cooper, B.; Kath, J. C.; Roberts, W. G.; Parsons, J. T. Cellular Characterization of a Novel Focal Adhesion Kinase Inhibitor. *J. Biol. Chem.* **2007**, *282* (20), 14845−52.

(9) Ott, G. R.; Cheng, M.; Learn, K. S.; Wagner, J.; Gingrich, D. E.; Lisko, J. G.; Curry, M.; Mesaros, E. F.; Ghose, A. K.; Quail, M. R.; Wan, W.; Lu, L.; Dobrzanski, P.; Albom, M. S.; Angeles, T. S.; Wells-Knecht, K.; Huang, Z.; Aimone, L. D.; Bruckheimer, E.; Anderson, N.; Friedman, J.; Fernandez, S. V.; Ator, M. A.; Ruggeri, B. A.; Dorsey, B. D. Discovery of Clinical Candidate CEP-37440, a Selective Inhibitor of Focal Adhesion Kinase (FAK) and Anaplastic Lymphoma Kinase (ALK). *J. Med. Chem.* **2016**, *59* (16), 7478−96.

(10) Shi, Q.; Hjelmeland, A. B.; Keir, S. T.; Song, L.; Wickman, S.; Jackson, D.; Ohmori, O.; Bigner, D. D.; Friedman, H. S.; Rich, J. N. A Novel Low-Molecular Weight Inhibitor of Focal Adhesion Kinase, TAE226, Inhibits Glioma Growth. *Mol. Carcinog.* **2007**, *46* (6), 488−96.

(11) Heinrich, T.; Seenisamy, J.; Emmanuvel, L.; Kulkarni, S. S.; Bomke, J.; Rohdich, F.; Greiner, H.; Esdar, C.; Krier, M.; Grädler, U.; Musil, D. Fragment-Based Discovery of New Highly Substituted 1H-Pyrrolo[2,3-b]- and 3H-Imidazolo[4,5-b]-Pyridines as Focal Adhesion Kinase Inhibitors. *J. Med. Chem.* **2013**, *56* (3), 1160−1170.

(12) Choi, H.-S.; Wang, Z.; Richmond, W.; He, X.; Yang, K.; Jiang, T.; Karanewsky, D.; Gu, X.-j.; Zhou, V.; Liu, Y.; Che, J.; Lee, C. C.; Caldwell, J.; Kanazawa, T.; Umemura, I.; Matsuura, N.; Ohmori, O.; Honda, T.; Gray, N.; He, Y. Design and synthesis of 7H-pyrrolo[2,3-d]pyrimidines as focal adhesion kinase inhibitors. Part 2. *Bioorg. Med. Chem. Lett.* **2006**, *16* (10), 2689−2692.

(13) Dao, P.; Smith, N.; Tomkiewicz-Raulet, C.; Yen-Pon, E.; Camacho-Artacho, M.; Lietha, D.; Herbeuval, J.-P.; Coumoul, X.; Garbay, C.; Chen, H. Design, Synthesis, and Evaluation of Novel Imidazo[1,2-a][1,3,5]triazines and Their Derivatives as Focal Adhesion Kinase Inhibitors with Antitumor Activity. *J. Med. Chem.* **2015**, *58* (1), 237−251.

(14) Ferguson, F. M.; Gray, N. S. Kinase Inhibitors: the Road Ahead. *Nat. Rev. Drug Discovery* **2018**, *17* (5), 353−377.

(15) Lin, A.; Giuliano, C. J.; Palladino, A.; John, K. M.; Abramowicz, C.; Yuan, M. L.; Sausville, E. L.; Lukow, D. A.; Liu, L.; Chait, A. R.; Galluzzo, Z. C.; Tucker, C.; Sheltzer, J. M. Off-Target Toxicity is a Common Mechanism of Action of Cancer Drugs Undergoing Clinical Trials. *Sci. Transl. Med.* **2019**, *11* (509), eaaw8412.

(16) Deng, X.; Yang, Q.; Kwiatkowski, N.; Sim, T.; McDermott, U.; Settleman, J. E.; Lee, J. D.; Gray, N. S. Discovery of a Benzo[e]-pyrimido-[5,4-b][1,4]diazepin-6(11H)-one as a Potent and Selective Inhibitor of Big MAP Kinase 1. *ACS Med. Chem. Lett.* **2011**, *2* (3), 195−200.

(17) Ferguson, F. M.; Ni, J.; Zhang, T.; Tesar, B.; Sim, T.; Kim, N. D.; Deng, X.; Brown, J. R.; Zhao, J. J.; Gray, N. S. Discovery of a Series of 5,11-Dihydro-6H-benzo[e]pyrimido[5,4-b][1,4]diazepin-6-ones as Selective PI3K-delta/gamma Inhibitors. *ACS Med. Chem. Lett.* **2016**, *7* (10), 908−912.

(18) Groendyke, B. J.; Powell, C. E.; Feru, F.; Gero, T. W.; Li, Z.; Szabo, H.; Pang, K.; Feutrill, J.; Chen, B.; Li, B.; Gray, N. S.; Scott, D. A. Benzopyrimidodiazepinone Inhibitors of TNK2. *Bioorg. Med. Chem. Lett.* **2020**, *30* (4), 126948.

(19) Wang, J.; Erazo, T.; Ferguson, F. M.; Buckley, D. L.; Gomez, N.; Munoz-Guardiola, P.; Dieguez-Martinez, N.; Deng, X.; Hao, M.; Massefski, W.; Fedorov, O.; Offei-Addo, N. K.; Park, P. M.; Dai, L.; DiBona, A.; Becht, K.; Kim, N. D.; McKeown, M. R.; Roberts, J. M.; Zhang, J.; Sim, T.; Alessi, D. R.; Bradner, J. E.; Lizcano, J. M.; Blacklow, S. C.; Qi, J.; Xu, X.; Gray, N. S. Structural and Atropisomeric Factors Governing the Selectivity of Pyrimido-

https://dx.doi.org/10.1021/acsmedchemlett.0c00338
ACS Med. Chem. Lett. 2021, 12, 30−38

benzodiazipinones as Inhibitors of Kinases and Bromodomains. *ACS Chem. Biol.* **2018**, *13* (9), 2438−2448.
(20) Ferguson, F. M.; Nabet, B.; Raghavan, S.; Liu, Y.; Leggett, A. L.; Kuljanin, M.; Kalekar, R. L.; Yang, A.; He, S.; Wang, J.; Ng, R. W. S.; Sulahian, R.; Li, L.; Poulin, E. J.; Huang, L.; Koren, J.; Dieguez-Martinez, N.; Espinosa, S.; Zeng, Z.; Corona, C. R.; Vasta, J. D.; Ohi, R.; Sim, T.; Kim, N. D.; Harshbarger, W.; Lizcano, J. M.; Robers, M. B.; Muthaswamy, S.; Lin, C. Y.; Look, A. T.; Haigis, K. M.; Mancias, J. D.; Wolpin, B. M.; Aguirre, A. J.; Hahn, W. C.; Westover, K. D.; Gray, N. S. Discovery of a Selective Inhibitor of Doublecortin Like Kinase 1. *Nat. Chem. Biol.* **2020**, *16*, 635−643.
(21) Deng, X.; Elkins, J. M.; Zhang, J.; Yang, Q.; Erazo, T.; Gomez, N.; Choi, H. G.; Wang, J.; Dzamko, N.; Lee, J. D.; Sim, T.; Kim, N.; Alessi, D. R.; Lizcano, J. M.; Knapp, S.; Gray, N. S. Structural Determinants for ERK5 (MAPK7) and Leucine Rich Repeat Kinase 2 Activities of Benzo[e]pyrimido-[5,4-b]diazepine-6(11H)-ones. *Eur. J. Med. Chem.* **2013**, *70*, 758−67.
(22) Cromm, P. M.; Samarasinghe, K. T. G.; Hines, J.; Crews, C. M. Addressing Kinase-Independent Functions of FAK via PROTAC-Mediated Degradation. *J. Am. Chem. Soc.* **2018**, *140* (49), 17019−17026.
(23) Tsherniak, A.; Vazquez, F.; Montgomery, P. G.; Weir, B. A.; Kryukov, G.; Cowley, G. S.; Gill, S.; Harrington, W. F.; Pantel, S.; Krill-Burger, J. M.; Meyers, R. M.; Ali, L.; Goodale, A.; Lee, Y.; Jiang, G.; Hsiao, J.; Gerath, W. F. J.; Howell, S.; Merkel, E.; Ghandi, M.; Garraway, L. A.; Root, D. E.; Golub, T. R.; Boehm, J. S.; Hahn, W. C. Defining a Cancer Dependency Map. *Cell* **2017**, *170* (3), 564−576.
(24) Taliaferro-Smith, L.; Oberlick, E.; Liu, T.; McGlothen, T.; Alcaide, T.; Tobin, R.; Donnelly, S.; Commander, R.; Kline, E.; Nagaraju, G. P.; Havel, L.; Marcus, A.; Nahta, R.; O'Regan, R. FAK Activation is Required for IGF1R-Mediated Regulation of EMT, Migration, and Invasion in Mesenchymal Triple Negative Breast Cancer Cells. *Oncotarget* **2015**, *6* (7), 4757−72.
(25) Pan, M. R.; Hou, M. F.; Ou-Yang, F.; Wu, C. C.; Chang, S. J.; Hung, W. C.; Yip, H. K.; Luo, C. W. FAK is Required for Tumor Metastasis-Related Fluid Microenvironment in Triple-Negative Breast Cancer. *J. Clin. Med.* **2019**, *8* (1), 38.
(26) Janes, M. R.; Zhang, J.; Li, L. S.; Hansen, R.; Peters, U.; Guo, X.; Chen, Y.; Babbar, A.; Firdaus, S. J.; Darjania, L.; Feng, J.; Chen, J. H.; Li, S.; Li, S.; Long, Y. O.; Thach, C.; Liu, Y.; Zarieh, A.; Ely, T.; Kucharski, J. M.; Kessler, L. V.; Wu, T.; Yu, K.; Wang, Y.; Yao, Y.; Deng, X.; Zarrinkar, P. P.; Brehmer, D.; Dhanak, D.; Lorenzi, M. V.; Hu-Lowe, D.; Patricelli, M. P.; Ren, P.; Liu, Y. Targeting KRAS Mutant Cancers with a Covalent G12C-Specific Inhibitor. *Cell* **2018**, *172* (3), 578−589.e17.
(27) Santana-Codina, N.; Chandhoke, A. S.; Yu, Q.; Malachowska, B.; Kuljanin, M.; Gikandi, A.; Stanczak, M.; Gableske, S.; Jedrychowski, M. P.; Scott, D. A.; Aguirre, A. J.; Fendler, W.; Gray, N. S.; Mancias, J. D. Defining and Targeting Adaptations to Oncogenic KRAS(G12C) Inhibition Using Quantitative Temporal Proteomics. *Cell Rep.* **2020**, *30* (13), 4584−4599.
(28) Han, K.; Pierce, S. E.; Li, A.; Spees, K.; Anderson, G. R.; Seoane, J. A.; Lo, Y. H.; Dubreuil, M.; Olivas, M.; Kamber, R. A.; Wainberg, M.; Kostyrko, K.; Kelly, M. R.; Yousefi, M.; Simpkins, S. W.; Yao, D.; Lee, K.; Kuo, C. J.; Jackson, P. K.; Sweet-Cordero, A.; Kundaje, A.; Gentles, A. J.; Curtis, C.; Winslow, M. M.; Bassik, M. C. CRISPR Screens in Cancer Spheroids Identify 3D Growth-Specific Vulnerabilities. *Nature* **2020**, *580* (7801), 136−141.
(29) Howe, G. A.; Xiao, B.; Zhao, H.; Al-Zahrani, K. N.; Hasim, M. S.; Villeneuve, J.; Sekhon, H. S.; Goss, G. D.; Sabourin, L. A.; Dimitroulakos, J.; Addison, C. L. Focal Adhesion Kinase Inhibitors in Combination with Erlotinib Demonstrate Enhanced Anti-Tumor Activity in Non-Small Cell Lung Cancer. *PLoS One* **2016**, *11* (3), No. e0150567.
(30) Tiede, S.; Meyer-Schaller, N.; Kalathur, R. K. R.; Ivanek, R.; Fagiani, E.; Schmassmann, P.; Stillhard, P.; Hafliger, S.; Kraut, N.; Schweifer, N.; Waizenegger, I. C.; Bill, R.; Christofori, G. The FAK Inhibitor BI 853520 Exerts Anti-Tumor Effects in Breast Cancer. *Oncogenesis* **2018**, *7* (9), 73.
(31) De Brabander, M. J.; Van de Veire, R. M.; Aerts, F. E.; Borgers, M.; Janssen, P. A. The Effects of Methyl (5-(2-thienylcarbonyl)-1H-benzimidazol-2-yl) Carbamate, (R 17934; NSC 238159), a New Synthetic Antitumoral Drug Interfering with Microtubules, on Mammalian Cells Cultured in vitro. *Cancer Res.* **1976**, *36* (3), 905−16.
(32) Chen, G.; Gao, C.; Gao, X.; Zhang, D. H.; Kuan, S. F.; Burns, T. F.; Hu, J. Wnt/beta-Catenin Pathway Activation Mediates Adaptive Resistance to BRAF Inhibition in Colorectal Cancer. *Mol. Cancer Ther.* **2018**, *17* (4), 806−813.

https://dx.doi.org/10.1021/acsmedchemlett.0c00338
ACS Med. Chem. Lett. 2021, 12, 30−38